Multi-Purpose Tool for Checking the Microfabrication Products

G. De Pasquale and A. Somà

Politecnico di Torino, Department of Mechanics
Corso Duca degli Abruzzi 24, 10129 Torino, Italy
giorgio.depasquale@polito.it, aurelio.soma@polito.it

ABSTRACT

This paper introduces a multi-purpose tool addressed to the microfabrication processes monitoring and material property measurement at the wafer level during both process development and manufacturing. Some procedures with high levels of automation and on-line controllability are introduced; the final goal is to provide compact algorithms for the real-time checking of building processes and material properties.

Keywords: MEMS, building processes, on-line control, material characterization.

1 INTRODUCTION

The on-line testing tool presented in this paper is the result of long-term studies about the interactions between the physical parameters involved in microfabrication processes and the properties of the material and of the structure of final products. Several fields of microstructural engineering were investigated in the past years by the authors and relevant results have been documented about the modeling, simulation and experimental validation of the most crucial properties of microdevices: microfluidics, structural interactions with fluids, electro-mechanical coupling, prediction and regulation of the dynamic response, residual material stress and strain, thermal effects, micromechanical fatigue, etc. The previous studies demonstrate that it is possible to calculate by equations or by simulations (e.g. with FEM) the constraints that are responsible of a specific observed behavior of a structure or sample; usually the constraint typologies are structural (geometry, clamped ends distribution, anchor losses, etc.), thermal (Joule effect, environment, fabrication heating and cooling, etc.), electric (bias, residual charge, etc.), tensional (residual stress, residual strain, etc) [1-4]. Up to now, the entity of the constraint has been predicted and estimated quantitatively by a previous testing of the behavior of dedicated samples and then applying a suitable model [5, 6]. Unfortunately this approach is only able to evaluate one constraint per time, because the interaction of multiple physical effects complicates a lot the models; consequently some discrepancies with the real coupled response may affect the predictions. Also, a lot of dedicated samples must be developed to accentuate the desired effects and make them measurable.

The tool described here is innovative in this sense; it is able to calculate the amount of the most important constraints acting on the products of microfabrication by measuring few simple parameters. Also, only two sample structures are used in the on-line testing by reducing the impact on the manufacturing process in terms of wafer area occupied and design time expense. This is possible by using dedicated modeling approaches which are able to uncouple the interactions between the physical constraints (e.g. thermal gradients and residual stress) on the same sample by few simple measurements. The results of the on-line testing can be used to control in real time two kinds of parameters: the main material constants and structural properties (i.e. Young module, thermal expansion coefficient, stress gradients, anchors shape, planarity and other strain-related properties, etc.) and the most effective manufacturing process parameters.

The multi-purpose tool exploits the optical strategy as it is contactless and provides a high sensitivity recording; the on-line testing is based on very few measurements in the static, dynamic and thermal fields, which provide the inputs for the calculation. The final goal of the tool is to minimize the cut-and-try approaches required by complicated processes involving several steps and, in an initial phase, several splitting to validate the best configuration. Also, the established running processes can be sustained by the self-assistance provided by this multi-purpose tool.

2 TEST STRUCTURES

Two typologies of test structures are used for the evaluation of material and process parameters: cantilevers and microbridges (Fig. 1).

Figure 1: Lateral drawing of two sample typologies.

The shape of the specimens is very simple to obtain and the area occupied on the wafer is considerably small. About the location of the samples on the wafer, it is preferable to

place the set of test structures in 3 or 4 different positions to capture the process variability on the whole area. Building processes involving mechanical actions (e.g. DRIE) or light emission (e.g. photolithography) may introduce differences in the material properties between the center and the periphery of the wafer due to the angle of incidence. Each type of test structures is replicated several times to obtain a set of cantilevers and microbridges with variable lengths. Figure 2 reports the optical detected image of the sets of cantilevers (left) and microbridges (right); the area occupied by each set is a square with about 500μm side. As indicated in Fig. 1, the most relevant geometrical parameters of the samples are the beam length (l), the beam width (w), the beam thickness (t) and the air gap thickness (g).

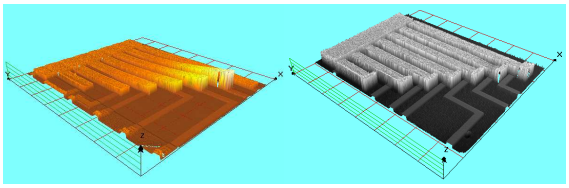

Figure 2: Optical image of the two sets of test structures.

3 ON-LINE CONTROL FACILITIES

The optical strategy was selected for the measurements due its high precision and repeatability, the fast response and the contactless of the detection. Also, this technique can be used for various types of measurements: profilometric, static detections, and dynamic measurements. The optical equipment is versatile and can be applied, as a checking stage, to almost all the building processes. The optical interferometry was used for the measurements presented in this work (Fogale Nanotech, ZoomSurf 3D), but other strategies are available at this purpose such as the laser technique. Usually the optical interferometry is more indicated for static and profile measurements, instead the laser techniques are functional to dynamic detections.

Additionally, some equipment is needed for the tests in temperature where a simple system for the heating control is required. In the case presented in this work, where only small dices were characterized, the temperature was increased by means of a Peltier cell with a PT100 temperature sensor (Fig. 3).

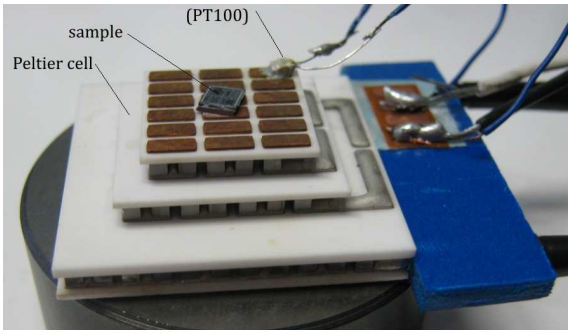

Figure 3: Temperature control system.

4 MATERIAL PROPERTIES

The effect of thermal expansion and contraction may alter the stress distribution in the material during the fabrication process; this effect is accentuated for multiple layered structures. The evaluation of some material properties by optical detection can be influenced by the presence of residual stress. This problem is accentuated for particular constraint configuration, as double clamping.

4.1 Young's module

The Young's module (E) is an indicator of the mechanical response of the material and should be controlled in those processes where additives are used. The pull-in voltage detection is the simplest way to measure E: the dynamic response analysis is also applicable, but more complicated post-processing of the measured data is necessary; nanoindentation techniques requires dedicated facilities that complicates the real-time checking.

In order to uncouple the effects of residual stress gradients and flexural response of the structure, the cantilever is used [7]. The possible residual strain of the material, which is usually exhibited as a beam curvature, may be accounted for as described in the following. The Osterberg-Senturia formulation [5] can be used to analytically calculate the Young's module from the experimental measurement of the pull-in voltage (V_{pi}) of a cantilever:

$$E = V_{pi}^2 \frac{\varepsilon_0 l^4}{4\gamma_1 g^3 t^3}\left(1+\gamma_2 \frac{g}{w}\right) \quad (1)$$

where ε_0 is the electric permittivity, γ_1=0.07 and γ_2=0.42. For curled cantilevers, the model presented by Gupta [8] can be used to include the curvature of the beam in the calculation; starting from the pull-in voltage measured on a curled cantilever ($V_{pi,c}$), the corresponding pull-in voltage of the flat cantilever is given by

$$\frac{V_{pi,c}}{V_{pi}} \cong 1+\frac{1}{2}\left(\frac{l^2}{gR}\right) \quad (2)$$

where R is the curvature radius, calculated as the inverse of the curvature.

The procedure described can be effectively used to characterize the Young's module at variable temperature; the same test can be repeated at different levels of temperature together with the further measurements, which are described in the following. This uncoupling strategy is very practical for those materials who exhibit significant variations of E with temperature.

4.2 Thermal expansion coefficient

Thermal properties of the material are described by the thermal expansion coefficient (α). It is possible to simplify a lot the determination of this parameter by using the relation between the thermal expansion of the material and the mechanical structural instability. In presence of multiple constraints (e.g. in microbridges), it was observed in the literature the effect of the thermomechanical buckling under compression, which is purely caused by the temperature increasing without application of external forces [9]. For ideal constraints this effect can be predicted by analytical or numerical models, like that one presented by the authors in [3].

The on-line characterization of α is based on the automatic heating of the microbridges present in the set of samples dedicated to check the material properties. The temperature is increased and monitored time by time by the sensor during the thermal expansion of the material that finally induces the structural buckling under the increasing axial force; the variation of the deflection velocity of the microbridge in the flexural mode due to the thermal-induced instability is detected by the optical instrumentation. From the buckling temperature, it is possible to determine the value of α for that material. This test is conducted at the same time on several samples of the set with variable lengths to improve the statistical confidence of the result.

A very well known formulation for the prediction of the critical load to induce the elastic instability phenomenon on a double clamped beam was introduced by Timoshenko [10]:

$$P_{\mathrm{cr}} = \frac{4\pi^2 EI}{l^2} \tag{3}$$

where I is the moment of inertia of the cross section of the beam ($I = wt^3/12$).

By indicating with T' the experimental value of the buckling temperature (i.e. the temperature at which the structural buckling occurs without any external force applied), the compressive force caused by the thermal expansion of the material at the buckling is

$$P_{\mathrm{t}} = \alpha\left(T' - T_0\right)EA \tag{4}$$

where T_0 is the reference (environment) temperature and A is the cross section area of the beam ($A = wt$). The structural-thermal instability condition is described by the equation

$$P_{\mathrm{t}} \pm \sigma_{\mathrm{r}} A = P_{\mathrm{cr}}\,. \tag{5}$$

In the above equation, the contribution of the residual stress is introduced (σ_{r} indicates the average stress of the cross section). The fabrication process may generate a residual stress in the material; depending on the technological process, the residual stress can be positive or negative and accelerate or retard the structural instability. The amount of the residual stress is strictly connected to the characteristics of the building process and is discussed in the next section. From Eqs. (3-5), the resulting expression to calculate the thermal expansion coefficient is

$$\alpha = \frac{4\pi^2 I}{l^2 A\left(T' - T_0\right)} \pm \frac{\sigma_{\mathrm{r}}}{E\left(T' - T_0\right)}\,. \tag{6}$$

5 RESIDUAL STRESS OF FABRICATION

Any manufacturing process introduces residual stress within the structures; many studies have been conducted to describe the effect of fabrication parameters such as baths composition, seed layer material properties, temperature and time of deposition, etc. on the final stress gradient. In general, it is difficult to predict the dynamic behavior of MEMS structures affected by the presence of nonuniform stress distribution; this is obtained with the following analytic model through the interpretation of the dynamic response of microbridges. The residual stress is introduced to explain the discrepancy between the measured value of resonance frequency and the theoretical expected value predicted by the Euler–Bernoulli formulation [1].

The axial residual stress component is not released in double clamped structures because of the hyperstatic configuration of the constraints; it is well known that the dynamic behavior involving deformed shapes orthogonal to the axial direction (transverse motions) is influenced by the axial load [11]. The stress-stiffening effect produced in double clamped structures by residual stress can be accounted for by using an elemental discretization of the structure based on the matrix formulation of the governing equation of a second order dynamic system. The stiffness matrix must be corrected by an additional stress-stiffening matrix representing a geometrical term. The final stiffness matrix [K] is defined as

$$\left[K\right] = \left[K_{\mathrm{e}}\right] + \left[K_{\mathrm{s}}\right] \tag{7}$$

where [K_{e}] is the standard elastic stiffness matrix calculated for the element geometry and [K_{s}] is the stress-stiffening matrix, which depends not only on the geometry but also on the initial internal stress. By modeling the microbridge with two discrete elements, as described in [1], the axial residual stress for the double clamped beam can be calculated from the first (ω_1) and the second (ω_2) natural frequencies, alternatively as

$$\sigma_{\mathrm{r}} = \frac{\theta_{1,2}}{\left(1-\nu\right)}\left(\frac{\rho l^2}{\beta_{1,2}^4}\omega_{1,2}^2 - \frac{\tilde{E}I}{Al^2}\right) \tag{8}$$

with $\theta_1 = 38.56$, $\beta_1 = 4.768$, $\theta_2 = 125.36$, $\beta_2 = 8.912$, where ν is the Poisson's coefficient, ρ is the density and $\tilde{E}$ is the Young's module corrected as in [5].

6 RESULTS

The experimental values of resonance frequency measured on two sets (black and white dots) of

microbridges with variable lengths ($w = 35\mu$m and $t = 2.9\mu$m) are reported in Fig. 4a with triangles. The results of numerical (circles) and analytic (squares) modeling of the structures in stress-relaxed conditions are not coincident, testifying the relevance of residual stress. From Eq. (8), the residual stress trend reported in Fig. 4b is obtained.

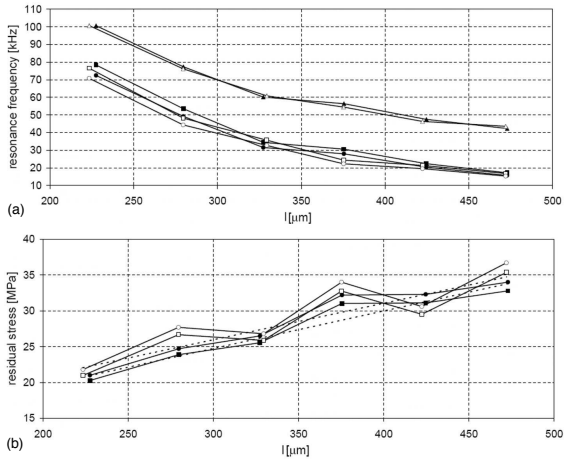

Figure 4: Resonance frequency (a) and residual stress (b) of two sets of microbridges.

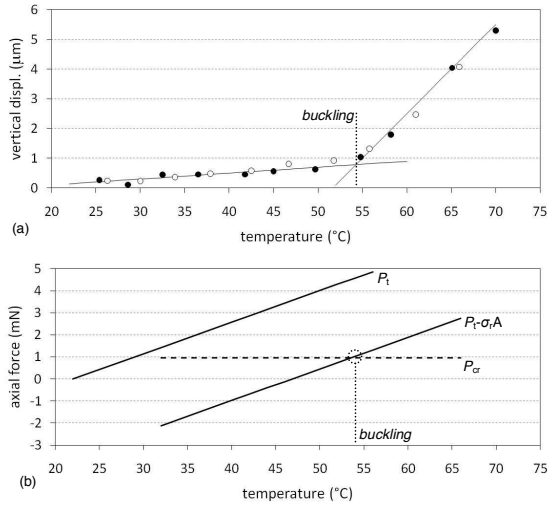

Figure 5: Measured vertical displacement of a microbridge under thermal load (a) and axial forces behavior (b).

The measured vertical displacement of a microbridge (central section) with $l = 540\mu$m, $w = 35\mu$m and $t = 2.9\mu$m is reported in Fig. 5a for increasing temperatures [3]. The structure exhibits a thermo-mechanical buckling at about 54.3°C, where a strong variation of the displacement velocity is present. From Eq. (3), the critical load inducing the axial instability is P_{cr}=0.948mN; if the residual stress σ_r=37MPa calculated before is introduced into the axial equilibrium equation, the thermal load inducing the buckling is obtained at 54.0°C that confirms the experimental results. The thermal load and the critical threshold are represented in Fig. 5b. Finally, the thermal expansion coefficient was determined by introducing in the Eq. (6) the residual stress calculated; the value $\alpha = 14.3 \cdot 10^{-6}$°C^{-1} was obtained.

REFERENCES

[1] G. De Pasquale and A. Somà, "Dynamic identification of electrostatically actuated MEMS in the frequency domain", Mechanical Systems and Signal Processing, 24 (6), 1621-1633, 2010.

[2] A. Somà, G. De Pasquale, E. Brusa and A. Ballestra, "Effect of residual stress on the mechanical behaviour of microswitches at pull-in", Strain, 46 (4), 358-373, 2010.

[3] E. Brusa, G. De Pasquale and A. Somà, "Characterization of thermo-mechanical coupling in gold microbridges", proc. Symposium of Design, Test, Integration and Packaging of MEMS/MOEMS (DTIP), Seville, Spain, 344-349, 2010.

[4] A. Somà and G. De Pasquale, "MEMS Mechanical Fatigue: Experimental Results on Gold Microbeams", Journal of Microelectromechanical Systems, 18 (4), 828-835, 2009.

[5] P.M. Osterberg and S.D. Senturia, "M-TEST: A test chip for MEMS material property measurement using electrostatically actuated test structures", Journal of Microelectromechanical Systems, 6 (2), 107-118, 1997.

[6] D.E. Lee, I. Hwang, C.M.O. Valente, J.F.G. Oliveira and D.A. Dornfeld, "Precision manufacturing process monitoring with acoustic emission", International Journal of Machine Tools and Manufacture, 46 (2), 176-188, 2006.

[7] A. Somà and A. Ballestra, "Residual stress measurement method in MEMS microbeams using frequency shift data", Journal of Micromechanics and Microengineering, 19, 095023, 2009.

[8] K.J. Gupta, "Electrostatic pull-in test structure design for in-situ mechanical property measurements of microelectromechanical systems (MEMS)", PhD dissertation, 1998.

[9] B.D. Jensen, K. Saitou, J.L. Volakis and K. Kurabayashi, "Fully integrated electrothermal multidomain modeling of RF MEMS switches", IEEE Microwave and wireless components letters, 13 (9), 2003.

[10] S. Timoshenko and J. Gere, "Theory of elastic stability", McGraw Hill, Tokyo, 1961.

[11] J.S. Przemieniecki, "Theory of matrix structural analysis", McGraw-Hill Book Company, New York, USA, 1968.